

**ZnO GROWTH MECHANISM AND
HETEROSTRUCTURES ON GaN AND DIAMOND**

TNEH SAU SIONG

UNIVERSITI SAINS MALAYSIA

2016

**ZnO GROWTH MECHANISM AND
HETEROSTRUCTURES ON GaN AND DIAMOND**

by

TNEH SAU SIONG

**Thesis submitted in fulfillment of the requirements
for the degree of
Doctor of Philosophy**

May 2016

ACKNOWLEDGEMENT

I would like to express my gratitude to my main supervisor Prof. Zainuriah Hassan as well as Assoc Prof Dr Saw Kim Guan, Dr Yam Fong Kwong and Prof Haslan Abu Hassan who have guided me in my research work. I am particularly grateful for the financial support from Universiti Sains Malaysia from a few research grants such as the FRGS and the short term research grants. I also wish to thank the staffs at the Nano-optoelectronics Laboratory who have helped me in various ways.

Thanks to my family who have cared and supported me throughout these years.

TABLE OF CONTENTS

	Page
ACKNOWLEDGEMENT.....	ii
TABLE OF CONTENTS.....	iii
LIST OF TABLES.....	viii
LIST OF FIGURES.....	ix
LIST OF ABBREVIATIONS.....	xiii
LIST OF SYMBOLS.....	xiv
ABSTRAK.....	xv
ABSTRACT.....	xvii
 CHAPTER 1 : INTRODUCTION	
1.1 Introduction to ZnO.....	1
1.2 Research background.....	2
1.3 Research Objectives.....	4
1.4 Originality of the research works.....	6
1.5 Outline of the thesis.....	7
 CHAPTER 2 : LITERATURE REVIEW	
2.1 Introduction.....	8
2.2 The growth techniques of ZnO and their nanostructures.....	8
2.2.1 Magnetron sputtering deposition.....	8
2.2.2 Chemical solutions.....	10
2.2.2(a) Spray pyrolysis.....	10
2.2.2(b) Sol-gel.....	11
2.2.2(c) Chemical bath deposition.....	12
2.2.3 Oxidation of metallic Zn.....	14
2.2.4 Solid-vapor phase deposition.....	15
2.2.5 Pulsed laser deposition.....	17

2.3	Doping and contacts of ZnO.....	18
2.4	Choice of substrates.....	20
2.5	ZnO heterojunctions.....	21
2.6	ZnO based UV photodetector.....	22

CHAPTER 3: MATERIALS AND CHARACTERIZATION PRINCIPLES

3.1	Materials.....	24
3.2	Sputtering target and metal sources.....	25
3.3	Characterization principles.....	26
3.3.1	X-Ray Diffraction.....	25
3.3.2	Scanning electron microscopy	28
3.3.3	Energy Dispersive Spectroscopy.....	28
3.3.4	Raman spectroscopy.....	29
3.3.5	UV-Vis Spectroscopy.....	30
3.3.6	Photoluminescence.....	32
3.3.7	Four point probe.....	33
3.3.8	Current-voltage measurements.....	35
3.3.9	Hall effect measurement with van de Pauw configuration	35

CHAPTER 4: METHODOLOGY

4.1	Introduction.....	39
4.2	Investigating the evolution of physical properties of Zn-ZnO.....	38
4.3	Growth of ZnO nanostructures.....	41
4.4	Investigation of Ni on ZnO structural properties and surface polar determination.....	42

4.5	Fabrication and investigation of ZnO-based heterojunctions and applications.....	44
4.5.1	Fabrication and investigation of the properties of ZnO/p-type GaN heterojunction	44
4.5.2	Fabrication and investigation of the properties of ZnO/p-type diamond heterojunction.....	46

**CHAPTER 5: RESULTS AND DISCUSSION
(INVESTIGATION ON GROWTH AND PROPERTIES DURING THE TRANSFORMATION OF Zn TO ZnO)**

5.1	Introduction.....	48
5.1.1.	First stage of thermal oxidation.....	48
5.1.2.	Second stage of thermal oxidation.....	63
5.1.3.	Growth process of Zn-ZnO thin film.....	74
5.2	Summary.....	81

**CHAPTER 6 : RESULTS AND DISCUSSION
(THE EFFECT OF THERMAL OXIDATION ON GROWING OF ZnO NANOSTRUCTURES SURFACE POLARITY OF ZnO THIN FILM)**

6.1	Introduction.....	84
6.2	The effect of flowing oxygen gas on the growth of ZnO nanostructures compared to annealing in an atmospheric ambience	84
6.2.1	Scanning electron microscopy analysis.....	84
6.2.2	Energy dispersion x-ray spectroscopy analysis.....	85
6.2.3	High Resolution XRD analysis.....	86
6.2.4	Photoluminescence analysis.....	87
6.3	The effect of oxidation durations on growing of ZnO nanostructures.....	89
6.3.1	Scanning electron microscopy analysis.....	89

6.3.2	High Resolution XRD analysis.....	90
6.3.3	Raman spectroscopy	91
6.3.4	Photoluminescence analysis	92
6.4	Investigation of possible determination of ZnO thin film surface polarity.....	95
6.5	Summary.....	100

**CHAPTER 7 : RESULTS AND DISCUSSION
(INVESTIGATION OF ZnO ON WIDE BANDGAP MATERIAL
HETEROJUNCTIONS)**

7.1	Introduction	102
7.1.1	Thermal oxidation effect of ZnO/p-type GaN heterojunction	102
7.1.2	UV illumination effect on ZnO/p-type diamond heterojunction.....	108
7.1.2.1	Structural and morphological properties of ZnO on type IIb diamond free standing substrate.....	110
7.1.2.2	Electrical properties of ZnO on type IIb diamond heterojunction.....	111
7.2	Summary.....	119

CHAPTER 8: CONCLUSION AND FUTURE WORK 121

8.1	Conclusions.....	121
8.2	Recommendations for future work.....	123

REFERENCES 124

LIST OF PUBLICATIONS 132

LIST OF TABLES

		Page
Table 2.1	The summary the selected growth techniques, precursors, morphological properties, and substrates for ZnO depositions.	23
Table 3.1	Some fundamental properties of ZnO	24
Table 5.1	XRD data of various samples obtained at different annealing durations	52
Table 5.2	Lattice constant c and a of ZnO with different annealing time	66
Table 5.3	Oxidation duration, Al contact resistance, and O/Zn ratio of the samples	71

LIST OF FIGURES

	Page	
Figure 2.1:	Schematic diagram of ZnO layer via sputtering method	9
Figure 2.2:	Typical experimental setup of ultrasonic spray pyrolysis method. 1. Carrier gas pipe, 2. Container, 3. Solution, 4. Ultrasonic nebulizer, 5. Heating system, 6. Nozzle, 7. Deposition chamber, 8. Substrate, and 9. Controller	11
Figure 2.3 :	Schematic diagram of sol-gel deposition methods a) spin-coating, b) dip-coating.	12
Figure 2.4:	A simple experimental setup for chemical bath deposition	13
Figure 2.5:	Schematic diagram of vacuum thermal evaporation process.	14
Figure 2.6:	Schematic of ZnO nanowires growth mechanism	15
Figure 2.7:	Schematic diagram of typical solid-vapor phase growth system	16
Figure 2.8 :	Schematic diagram of a pulsed laser deposition system.	17
Figure 2.9:	Schematic diagram of the basic ZnO homojunction..	21
Figure 2.10:	The optical images of a) Zn-polar, b) O-polar surface after etching	23
Figure 3.1:	Crystal structure of wurzite ZnO	25
Figure 3.2	Principle of Bragg's diffraction	27
Figure 3.3	Schematic diagram for the different types of scattering in Raman spectroscopy.	30
Figure 3.4:	Schematic diagram of a double beam UV-Vis spectrometer.	31
Figure 3.5:	Schematic diagram of a typical PL setup	33
Figure 3.6:	Schematic diagram of PL process	33
Figure 3.7:	Schematic diagram of four point probe.	34
Figure 3.8:	A typical current-voltage measurement set up.	35
Figure 3.9:	Schematic diagram of Hall effect setup..	36

Figure 3.10:	Metal contact geometry for van de pauw method a) preferred geometry, b acceptable geometry	37
Figure 4.1:	Flow chart of growth and characterizations for ZnO layer.	40
Figure 4.2:	Flow chart of growth and characterizations of ZnO nanostructures.	42
Figure 4.3:	Flow chart summarizes the experiment and characterizations procedure in determining the polarity of ZnO thin film.	43
Figure 4.4:	Simplified flow chart shows the study of the oxidation effect of ZnO/GaN heterojunctions.	45
Figure 4.5:	Schematic diagram of the heterojunction with top and side view. (Note that the diameter of the contact is 1mm.)	47
Figure 4.6:	Flow chart of studying characteristics of ZnO/diamond heterojunction.	47
Figure 5.1:	SEM micro-images for the samples with oxidation duration (a) 0 minutes (as deposited) , (b) 1,(c) 2 ,(d) 3,(e) 4, (f) 5, and (g) 6 minutes. The inset show higher magnification for the corresponding image. The inset scale bar is 1 micron	49
Figure 5.2:	(a) XRD patterns of samples with various oxidation durations; (b) enhanced XRD patterns to show the ZnO (100) peak for samples with oxidation durations 4 – 6 minutes.	51
Figure 5.3:	(a) Relative intensity of the ZnO (002) peak, (b) d-spacing, and (c) grain size of ZnO with oxidation time..	54
Figure 5.4:	(a) The change in resistivity for the samples with oxidation time, (b) FWHM of the ZnO (002) peak with resistivity of the samples.	57
Figure 5.5:	Optical transmittance of the samples in the range of a) 300 – 800 nm, b) 360 – 400 nm.	58
Figure 5.6:	Room temperature PL spectra of samples with different oxidation durations	59
Figure 5.7:	a) I_{uv}/I_{green} ratio , b) PL optical bandgap vs oxidation durations.	61
Figure 5.8 :	I-V characteristics of Al contacts on the samples	62
Figure 5.9:	Room temperature Raman spectra of the samples	62

Figure 5.10 :	XRD patterns of samples (a) as-deposited metallic Zn, (b) annealed with different durations; the peaks indicate that all the Zn has been converted to ZnO.	64
Figure 5.11:	Distribution of relative intensity, $i(002)$ with different annealing times	65
Figure 5.12:	SEM micrograph showing the morphology of samples for different annealing durations: a) as deposited, b) 15, c) 30, d) 45, e) 60 minutes.	68
Figure 5.13:	Transmission spectra of the samples with different annealing time. The inset shows transmittance values versus surface RMS roughness (nm).	69
Figure 5.14:	Room temperature PL spectra of samples	69
Figure 5.15:	I-V characteristics of non-annealed Al ohmic contacts on ZnO	71
Figure 5.16:	The characteristics of contact resistivity versus O/Zn ratio .	73
Figure 5.17:	The relation between ratio c/a and resistivity of sample with various oxidation durations.	72
Figure 5.18:	Room temperature Raman scattering spectra of the samples	74
Figure 5.19:	The ratio of transformation for various oxidation durations	76
Figure 5.20:	The activation energy with oxidation durations. The first point represents the activation energy for 1 to 2 min of annealing and so on. The last point represents the estimated activation energy for 6 to 15 min of annealing.	80
Figure 5.21:	Optical transmittance and I_z as function of annealing duration for various samples.	81
Figure 5.22:	The relationship of I_z vs optical transmittance.	81
Figure 6.1:	SEM images of ZnO films. (a) Sample A - annealing in atmospheric ambience only and (b) Sample B - annealing with O_2 flow rate of 4 Lmin^{-1}	85
Figure 6.2:	EDS spectrum of sample B. The ratio shows the atomic weight percentage for atoms of Zn and O.	86
Figure 6.3:	Typical XRD diffraction patterns of sample.	87
Figure 6.4:	PL spectra of polycrystalline ZnO films for different annealing conditions. Sample A (without O_2 flow) and sample B (with O_2 flow).	88

Figure 6.5:	SEM images of samples annealed for duration of a) 40, b) 80, and c) 120minutes.	89
Figure 6.6:	XRD patterns of samples annealed for duration of a) 40, b) 80, and c) 120 minutes.	90
Figure 6.7:	Raman spectra for the samples annealed for duration of 40 and 120 minutes.	91
Figure 6.8:	Photoluminescence spectra of ZnO nanostructure samples	92
Figure 6.9:	Photoluminescence spectra of blue luminescence of the samples	93
Figure 6.10:	The schematic diagram of the possible mechanisms for occurrence of native defect, interstitial zinc.	95
Figure 6.11:	I – V measurements of Ni contacts on ZnO thin film a) before annealing, (b) after annealing at 800oC and, XRD phase analysis patterns c) before annealing after annealing at 800°C.	96
Figure 6.12:	I – V measurements of the Ni contacts on (a) Zn-polar surface before annealing; (b) Zn-polar surface after annealing; (c) O-polar surface before annealing; (d) O-polar surface after annealing. (The inset in (a) and (c) show morphology images, and the inset scale bar = 10um) .	97
Figure 6.13:	XRD patterns of the Ni contacts on (a) Zn-polar surface pre-annealed; (b) Zn-polar surface post-annealed; (c) O-polar surface pre-annealed; (d) O-polar surface post-annealed.	98
Figure 7.1:	SEM images of ZnO a) as deposited b) oxidized with O ₂ , and GaN surface c) as deposited, d) oxidized.	102
Figure 7.2:	Room temperature PL spectra of the heterojunctions. Inset shows the cross section of the heterojunction.	103
Figure 7.3 :	a)XRD pattern of the ZnO/GaN heterojunction as deposited, b)XRD pattern of annealed ZnO/GaN	105
Figure 7.4:	I-V measurements of Al contacts on ZnO and Pd contacts on GaN.	106
Figure 7.5:	I-V measurements of the heterojunction a) as-deposited, b) after oxidation. The inset shows the ZnO/GaN heterojunction configuration.	106
Figure 7.6:	The draft of the ZnO/GaN heterojunction band diagram: (a) as-deposited, (b) oxidized in O ₂ ambient.	107

Figure 7.7:	a) Raman spectrum of the type IIb diamond, b) XPS spectrum to indicate the presence of boron by observed B KLL peak at the kinetic energy range 176-184 eV.	109
Figure 7.8:	a) XRD pattern of heterojunction, b) FESEM micro-image of as sputtered ZnO thin film.	110
Figure 7.9:	Ohmic behavior of In and Ni metal contacts on ZnO and type IIb diamond, respectively after annealing for 3 minutes.	111
Figure 7.10:	I-V measurements of ZnO / type IIb diamond heterojunction under dark and UV illumination condition. (The inset is showing the spectrum of UV source.)	112
Figure 7.11:	Figure 8.11: Threshold voltage for (a) dark condition, (b) UV illumination, reverse breakdown voltage for (c) dark condition, (d) UV illumination	113
Figure 7.12:	Ln current versus bias voltage for a) dark condition, b) UV illumination.	118
Figure 7.13:	The ratio of I_{UV}/I_{dark} in the range of forward current.	119

LIST OF ABBREVIATIONS

CVD	Chemical vapour deposition
EDS	Energy dispersive spectroscopy
NBE	Near band edge emission
PL	Photoluminescence
RF	Radio frequency
SEM	Scanning electron microscope
UV	Ultraviolet
UV-VIS	Ultraviolet-Visible
XPS	X-ray photoelectron spectroscopy
XRD	X-ray diffraction

LIST OF SYMBOLS

a	Lattice constant
c	Lattice constant
d	Distance
I	Current
I_S	Saturation current
k	Boltzmann's constant
m_o	Electron mass
m^*	Effective mass
R_H	Hall coefficient
R_s	Sheet resistance
T	Absolute temperature
V	Voltage
V_H	Hall voltage
S	Sensitivity
ϵ_o	Absolute dielectric constant
θ	Incident/Diffraction angle
λ	Wavelength

MEKANISME PERTUMBUHAN ZnO DAN HETEROSTRUKTUR ATAS GaN DAN INTAN

ABSTRAK

Dalam penyelidikan ini, sifat-sifat fizikal nanostruktur ZnO dan peranti yang berkaitan dikaji. Yang pertama, pertumbuhan melalui transformasi zink kepada zink oksida melalui pengoksidaan haba dibincangkan. Zn didapati menukar sepenuhnya kepada ZnO selepas penyepuhlindapan selama 15 minit. Data belauan sinar-x (XRD) itu menunjukkan tenaga permukaan minimum adalah ZnO (002) < ZnO(100) < ZnO(101). Jurang jalur optik sampel ZnO di dapati berada di jurang 3.19 – 3.25 eV. Penbandingan pancaran pinggir jalur dekat ultraungu (UV) dan hijau di dalam analisis fotoluminesen juga di bincangkan. Tenaga pengaktifan bagi proses ini adalah di dalam jurang 76-124 kJ/mol iaitu bersepadan dengan nilai migrasi bagi celahan Zn, kekosongan Zn, celahan O dan kekosongan O. Dengan membandingkan nilai-nilai tenaga pengaktifan bagi kecacatan yang kerap terdapat dalam ZnO dalam laporan dengan nilai yang dikira daripada XRD, adalah didapati proses transformasi ini disebabkan oleh kecacatan tersebut. Dengan membandingkan keputusan XRD dan penghantaran, transformasi daripada Zn kepada ZnO adalah didapati merupakan proses lapisan demi lapisan. Nanostruktur ZnO polihablur juga dapat dihasilkan daripada logam Zn melalui pengoksidaan haba bagi keadaan sepuh lidap yang berlainan. Corak XRD menunjukkan ZnO polihablur ini adalah berkualiti tinggi. Taburan nano-dawai dan nano-kepingan ini bergantung kepada gas oksigen dan juga tempoh sepuh lidap. Dengan menggunakan pengukuran XRD dan arus-voltan (I-V), polariti permukaan filem nipis ZnO dapat ditentukan. Selepas disepuh lindap pada suhu 800°C, filem nipis ZnO menunjukkan perubahan daripada sifat ohmik kepada

retifikasi yang menunjukkan permukaan Zn-terpenggal. Sifat rektifikasi yang didapati pada filem nipis ZnO adalah disebabkan oleh pembentukan nikel zink oksida. Pemendapan filem nipis ZnO di atas p-GaN komersial menunjukkan sifat simpangan p-n. Ciri I-V menunjukkan sifat rektifikasi bagi heterosimpang n-ZnO/p-GaN sebelum pengoksidaan haba. Walaubagaimana pun, sifat I-V yang berlainan didapati selepas pengoksidaan haba disebabkan oleh penghasilan lapisan antara muka Ga_2O_3 di antara heterosimpang ZnO/GaN yang menghasilkan telaga keupayaan untuk menghalang pergerakan elektron daripada ZnO kepada GaN semasa dalam keadaan pincang depan. Pemendapan ZnO atas intan juga menunjukkan sifat heterosimpang p-n. Pengukuran I-V menunjukkan perubahan sifat elektrik apabila di dalam keadaan gelap dan terdedah kepada cahaya ultra-lembayung (UV). Dengan menggunakan model yang mudah, perubahan tahap tenaga penderma sebanyak 50 meV telah berpindah berdekatan dengan paras tenaga konduksi ZnO. Perubahan voltan ambang dapat dianggarkan (0.4V) dan didapati ianya setanding dengan keputusan eksperimen. Seterusnya, kepekatan penerima bagi intan didapati sebagai $2.82 \times 10^{17} \text{ cm}^{-3}$ dan faktor kepekatan adalah 3.

ZnO GROWTH MECHANISM AND HETEROSTRUCTURES ON GaN AND DIAMOND

ABSTRACT

In this study, the physical properties of ZnO nanostructures and related devices have been investigated. Firstly, the growth via transformation of zinc to zinc oxide by thermal oxidation was discussed. The Zn completely has been found to transform to ZnO after 15 min of annealing. The x-ray diffraction (XRD) data suggest that the minimum surface energy of ZnO (002) < ZnO(100) < ZnO(101). Optical band gap of ZnO samples have been deduced in the range of 3.19 – 3.25 eV. The comparison of ultraviolet (UV) near band edge and green emissions in photoluminescence (PL) analysis has also been discussed. The activation energies of this process are in the range of 76- 124 kJ/mol which correspond to the range of migration values for Zn interstitials, Zn vacancies, O interstitials and O vacancies. By comparing the reported values of the activation energy of these defects commonly found for ZnO in literature and the calculated values from XRD, it is observed that the transformation process can be attributed to these defects. By comparing the XRD and transmittance results, this transformation from Zn to ZnO is pre-dominantly a layer-by-layer process. Polycrystalline ZnO nanostructures were also produced from metallic Zn by dry thermal oxidation method at different annealing conditions. The XRD spectrum shows that the polycrystalline ZnO films are of good quality. The distributions of nano-wires and nano-sheets depend on oxygen gas concentration and also on the duration of annealing. Using XRD and current-voltage (I-V) measurements, the surface polarity of the zinc oxide thin film can be determined.

After annealing at 800°C, the ZnO thin film shows a conversion from Ohmic to rectifying behavior which is indicative of a Zn-terminated surface. The rectifying behavior observed on the ZnO thin film is associated with the formation of nickel zinc oxide. The deposition of ZnO thin films on commercial p-type GaN is observed to demonstrate p-n junction properties. The I-V characteristics showed a rectifying behavior of the n-ZnO / p-GaN heterojunction before thermal oxidation. However, a different I-V behavior was observed after thermal oxidation due to the formation of Ga₂O₃ as an interfacial layer between ZnO/GaN heterojunction, creating a potential well to impede the electrons movement from ZnO to GaN during forward bias. The deposition of ZnO thin films on diamond was also observed to demonstrate p-n heterojunction behavior. The I-V measurements showed a change in electrical behavior under dark and UV exposure. Using a simple model, the donor level of 50 meV shifted closer to the conduction energy level of ZnO. The threshold voltage changes (0.4 V) could be estimated and was found to be consistent with the experimental results. Subsequently, the concentration of acceptor carriers of diamond and the sensitivity factor of the device were determined to be $2.82 \times 10^{17} \text{ cm}^{-3}$ and 3, respectively.

CHAPTER 1

INTRODUCTION

1.1 Introduction to ZnO

Zinc oxide (ZnO) is an oxide semiconductor from group II-VI materials. It possesses a hexagonal wurtzite structure and is relatively non-toxic. Due to the superior properties such as direct wide bandgap of 3.3 eV and a large exciton binding energy of 60 meV at room temperature, ZnO has been studied extensively and widely used in optoelectronic applications, particularly blue and ultra-violet optical devices (Jagadish et al., 2006). By contrast, silicon with a narrow and indirect band gap is not suitable for specific applications such as emitting blue and ultra-violet light. Currently, ZnO is used for applications such as sensors, transparent oxides, solar cells and varistors. ZnO has also the ability to grow into single crystal substrates, which will be tremendously useful for optical and electronic applications. There are several deposition methods to produce ZnO layers or thin films. The most popular methods that can be found in literature are sputtering, wet chemical, thermal evaporation, molecule beam epitaxy, chemical vapor deposition and atomic layer deposition. As cost effectiveness is one of the important factors in successful commercialization, it is fortunate that the fabrication of ZnO is a simple and straight forward process, moreover, this semiconductor is relatively free from toxic waste products.

The ability of ZnO to grow into various forms of nanostructures has added an advantage to its properties. Nanostructured semiconductors have attracted the attention of researchers owing to the influence of their surface morphology, nanoscale dimension, quantum confinement and tunneling transport, which often exhibit unique functional and enhanced properties as compared to their bulk

counterparts or thin films. Among these interesting features, the high ratio of surface to volume particularly received enormous attention, since it can increase the sensitivity of sensors. In order to grow well-array nanostructures, a metal catalyst such as Au or Ag is sometimes needed to lower the temperature required to grow.

As-grown ZnO is intrinsically n-type. It typically exhibits n-type conductivity although the source of electrons contributing to the n-type conductivity has not been conclusively identified. Zinc interstitials, oxygen vacancies, hydrogen and hydrocarbonates have been suggested as possible defects that contribute to the generation of donor carriers. The difficulty to grow a stable p-type ZnO is thus still a challenging task for researchers. Thus the fabrication of ZnO-based homojunctions is difficult. An alternative way to solve this problem is to introduce another p-type semiconductor such as gallium nitride or diamond to replace p-type ZnO.

1.2 Research background

The motivation for this study comes from various current issues that involve ZnO. Besides the major problems of unstable p-type electrical properties of ZnO (Ngo et al., 2011) , there is a lack of understanding about ZnO such as the growth mechanisms from Zn to ZnO layer. In particular, the progressive change of phase from Zn to ZnO and the associated physical properties remain unclear. Existing literature usually report on the physical properties of the final stage in the oxidation changes from Zn to ZnO. For instance, the previous studies of Wang et al. and Cho et al. report the physical properties at final stage of thermal oxidation of ZnO with polycrystalline Zn as the starting layer (Wang et al., 2003, Cho et al., 1999). The intermediate stage has not been reported on these studies. To investigate the intermediate stage, the (0002) crystalline plane of metallic Zn can provide useful

information. The intermediate stage of oxidation is also very useful to give insights on crystal growth.

ZnO is also known for its ability to grow as nanostructures. Most of the previous studies involve several experimental parameters such as deposition temperature, metal catalysts and types of substrates (Chen et al., 2010, Kumar et al., 2012, Khajavi et al., 2012). However, although the effect of oxygen addition on ZnO nanostructure growth and properties is important it is relatively unreported.

The use of ZnO in optoelectronic devices is very much related to its surface polarity. ZnO has a wurtzite structure but the ratio of its lattice parameters $c:a$ is 1.602. This ratio is lower than that for perfectly hexagonally close-packed atoms which is 1.633. The smaller ratio of the lattice parameters and the ionic nature of the Zn-O bond as well as the lack of inversion symmetry results in a net dipole moment along the c -axis of the unit cell. While the dipole moments cancel each other in the bulk they cause equal and opposite bound polarization charges on the Zn-polar and O-polar surfaces. Thus the surfaces of c -plane ZnO can exist as Zn- or O-terminated. Ohnishi *et al.* suggested that the surface of ZnO thin film is O-terminated. Sasaki *et al.*, (2005) however suggested that the polarity of ZnO thin films depend on the growth parameters such as temperature. The surface polarity is important because it will exhibit different electrical properties and chemical resistance ability (Endo *et al.*, 2007). Thus it is crucial to identify the surface polarity of ZnO. Two known methods of identifying the surface polarity are the co-axial impact collision ion scattering spectroscopy (CAICISS) (Ohnishi *et al.*, 1998) and etching with acid solutions (Endo *et al.*, 2007, Van *et al.*, 1991, Hupkes *et al.*, 2012). Both these methods have certain limitations. The former is a complicated and expensive system while the latter involves an uncontrollable etching rate and irreversible damage of ZnO surface.

Since the depth of a typical etch pit could be more than 1 μm , the latter method is also unsuitable for ZnO thin films as it can cause the film to delaminate.

There is a current research interest in ZnO-based p-n junction. Previous reports include Schottky photodiode on c-plane single crystal ZnO and epitaxial thin film as well as p-n homojunctions involving mono-doping with group V elements such as Sb, N, P, and As. A common problem of using ZnO-based devices is the intrinsic n-type conduction of ZnO due to the effect of self-compensation resulting in acceptor carriers in ZnO being easily compensated. Another challenge is the low solubility of dopants. Other problems in fabricating p-type ZnO are associated with the so-called aging effect where the ZnO material subsequently reverts to n-type conductivity. One of the motivations of this work is to replace p-type ZnO with a stable p-type material such as magnesium doped GaN or boron-doped diamond.

1.3 Research Objectives

The research work of this project mainly focuses on the study of diverse fundamental aspects of the ZnO. Prior to the ZnO device fabrication stage, the basic characteristics of ZnO need to be examined, therefore, the project starts from the investigation of ZnO physical properties obtained from simple oxidation of metallic Zn and growth of ZnO nanostructures at different annealing conditions. Based on various optical, structural and electrical properties collected from experimental results, eventually allows the subsequent study on the surface polarity of ZnO. All these fundamental properties provide a better understanding in the fabrication of heterostructures on GaN and diamond.

The research objectives of this study are:

- a) To investigate the characteristics of thin films associated with the progressive change of phase as metallic Zn is oxidized to ZnO due to various annealing durations;
- b) To investigate ZnO nanostructure growth in an oxygen ambient;
- c) To find an alternative method to determine the surface polarity of ZnO thin films;
- d) To investigate the properties of heterojunctions consisting of ZnO and other wide bandgap materials such as GaN and diamond

To achieve the objectives, this study is divided into four main parts:

- a) The study of the thermal annealing effects on the transformation from metallic Zn to ZnO.

An experiment is carried out to investigate the evolution of conversion of metallic Zn layer to ZnO in term of annealing durations. Various types of characterizations have been used to study the fundamental characteristics such as surface morphology, optical, structural, and electrical properties of the samples subject to different conditions of annealing. The results will allow researchers to have a better understanding about the formation and physical properties of the different phases of Zn, Zn-ZnO, and ZnO.

- b) The study on the growth of ZnO nanostructures in oxygen ambient.

The growth of catalysis-free ZnO nanostructures is studied in relation to the presence of oxygen ambient. A comparison between rich and poor oxygen content ambient will be done with a focus on annealing durations in

rich oxygen content ambient. The results will provide information about the distributions and the types of ZnO nanostructures.

c) Investigation of possible determination of ZnO thin film surface polarity

A possible method of determining the surface polarity will be investigated with a focus on structural and electrical properties. Differences in the Zn-polar and O-polar surfaces could indicate an alternative and easier method to determine surface polarity of ZnO thin films.

d) The fabrication and investigation of heterojunctions from ZnO and other wide bandgap materials

Heterojunctions are fabricated using ZnO and other wide bandgap materials. After fabrication, the physical characteristics especially electrical properties of the ZnO heterojunctions are investigated. The selected p-type semiconductors were p-type GaN and diamond that contains boron. The physical characteristics of thermal effects on ZnO /GaN heterojunction as well as ultra-violet illumination effect on ZnO/ diamond heterojunction will be studied. A theoretical explanation is proposed regarding the changes in the electrical properties.

1.4 Originality of the research work

- 1) New insight on the evolution of oxidation stages from metallic Zn to Zn-ZnO aggregate and finally to ZnO forms part of this study. Most studies on ZnO ignored the 'intermediate' stage where Zn and ZnO exist together.

- 2) Propose a new method in analyzing and determining the surface polarity of ZnO thin film.
- 3) Explore the annealing effect on electrical properties of ZnO/GaN heterojunction at high temperature.
- 4) First time to study and report the characteristics of ZnO/diamond heterojunction upon exposure to UV illumination.

1.5 Outline of the thesis

This thesis is presented as follows:

Chapter 2 consists of literature review of common methods of growing ZnO thin films and nanostructures, contacts on ZnO.

Chapter 3 covers the principles of the characterization methods used in this work.

Chapter 4 discusses the methodology involved in this work.

Chapter 5 contains the results and discussion of the investigation of the evolution of Zn-ZnO phase.

Chapter 6 presents the results and discussion of the effect of oxygen gas on the growth of ZnO nanostructures and determining the surface polarity of ZnO thin films.

Chapter 7 discusses the results of ZnO based heterojunctions.

Chapter 8 is the summary of this work and proposes future work related to this study.

CHAPTER 2

LITERATURE REVIEW

2.1 Introduction

This chapter presents an overview of the growth techniques of ZnO and their nanostructures, doping of ZnO and making contacts on ZnO, substrate candidate, ZnO heterojunction and ZnO related UV photo-detector.

2.2 The growth techniques of ZnO and their nanostructures

ZnO can be produced via various simple deposition or growth techniques such as magnetron sputtering, chemical solutions, oxidation from metallic Zn, solid-vapor phase deposition, and pulsed laser deposition. These techniques are discussed as follows.

2.2.1 Magnetron sputtering deposition

Magnetron sputtering is widely employed to fabricate ZnO thin films due to its flexibilities in the control of composition and microstructure (Hoon et al., 2011). Figure 2.1 shows the schematic diagram of sputtering working principle to coat ZnO layers. The vacuum chamber has to be pumped to 10^{-6} Pa before flowing an inert gas such as Ar to create a plasma. When the active plasma has been created, Ar^+ ions collide with the target when a high voltage difference between the cathode and the anode is applied using a power supply. This bombardment process will cause the Zn ions to be removed from the target and subsequently to make a layer of coating on the surface of substrate. Usually, a magnetron (attached with the target) is used to improve the efficiency of the ZnO layer formation. While a metallic Zn target is

used, a reactive gas such as O_2 is needed in the sputtering chamber to form a ZnO layer (Lee et al., 2002).

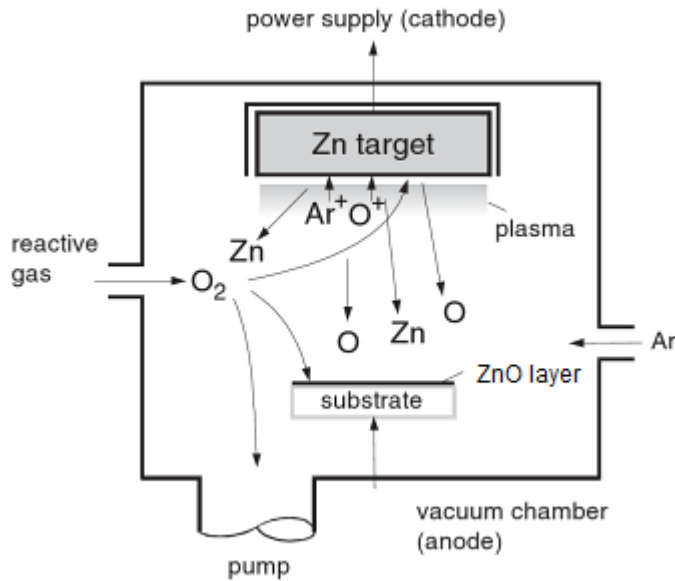


Figure 2.1 Schematic diagram of ZnO layer via sputtering method (Klaus et al., 2008).

The type of sputtering systems can be categorized as direct coating (DC) or radio frequency (RF), depending on the electrical properties of target materials. Zn metallic and ceramic ZnO targets use in both the DC sputtering and RF sputtering systems (Besleaga et al., 2012, Houng et al., 2012, Li et al., 2012, Lee et al., 2012). When a Zn target is used, the sputtered Zn thin film is usually subject to oxidation to fabricate a ZnO thin film. A range of temperature between 300 – 1000°C is needed (Cho et al., 1999 , Wang et al., 2003). Basically, conductive targets can be used in both DC and RF systems, and non-conductive targets can be used in the RF sputtering system only. However, the ceramic ZnO target still can be used in DC sputtering system to coat ZnO thin film. The influences of deposition parameter can directly changes the quality of ZnO thin film. Reports of successful ZnO thin films

by RF sputtering using a ZnO target have been used (Schropp ETAL., 1989, Wang et al., 2004 ,Lin et al., 2004).

2.2.2 Chemical solutions

Chemical solution methods received a good attention from researcher due to low productions cost and environmental friendly process. Another benefit of this deposition method allow to adding another precursors for doping or alloying process. Chemical solution methods to grow ZnO (thin films or nanostructures) such as spray pylorysis, sol-gel, and chemical bath depositions are widely reported in journals.

2.2.2(a) Spray pyrolysis

Spray pyrolysis or chemical spray pyrolysis can be used to deposit ZnO layers (Alver et al., 2007). The pyrolysis process takes place with a minimum deposition temperature of 450°C. This pyrolysis process will decompose the organic precursor without the present of oxygen. There is an ultrasonic nebulizer that is used to control the size of liquid droplets during deposition. Figure 2.2 shows the typical setup of spray pyrolysis.

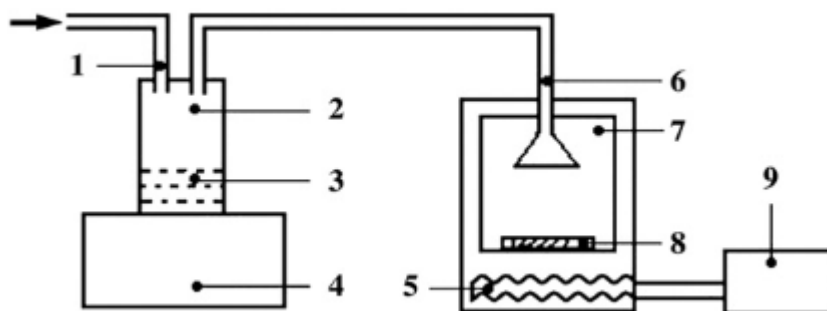


Figure 2.2 Typical experimental setup of ultrasonic spray pyrolysis method. 1. Carrier gas pipe, 2. Container, 3. Solution, 4. Ultrasonic nebulizer, 5. Heating system, 6. Nozzle, 7. Deposition chamber, 8. Substrate, and 9. Controller (adapted from Zhang et al., 2007).

The organic precursor to coat ZnO materials is usually zinc acetate which commonly occurs in the dehydrate form, $\text{Zn}(\text{O}_2\text{CCH}_3)_2(\text{H}_2\text{O})_2$. The carrier gas (Ar) brings the small (source) droplets from the liquid surface during the ultrasonic vibration. The source carried by the Ar gas goes through a nozzle and distribute evenly before reaching the surface of the substrate. The intended material will be thus deposited.

2.2.2(b) Sol-gel

ZnO materials also can be prepared by sol-gel method. The main feature of the sol-gel method is preparing a gel-like chemical solution with the zinc ion complex. Spin-coating and dip-coating are depositions usually performed in sol-gel method. Figure 2.3 shows the schematic diagram of two sol-gel deposition methods which are the spin-coating and dip-coating.

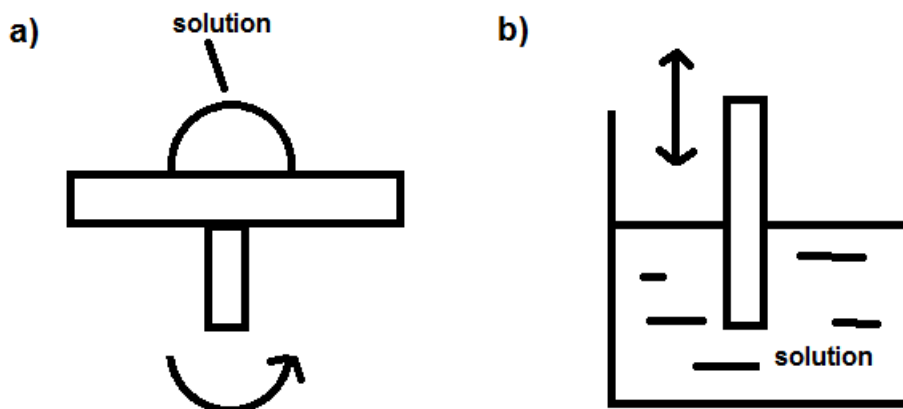


Figure 2.3: Schematic diagram of sol-gel deposition methods a) spin-coating, b) dip-coating.

The solvents of this sol-gel can be organic liquid (ethanol) and non-organic liquid (water) (Casanova et al., 2011). The stabilizer such as ethanolamine (MEA), or diethanolamine (DEA) is used to enhance the uniformity of the coating. Spin-coating (Figure 2.3a) with high speed rotating can distribute the solution on the substrate to become a thin film due to the rotating force (Sahoo et al., 2010, Wang et al., 2009). The thin film is then annealed. Dip-coating with a dipping speed can make the solution stick on the substrate evenly (Nain et al., 2010, Casanova et al., 2011). Both techniques allow controlling the thickness of layers by repeating the process with certain sol-gel recipes. The following annealing processes allow the chemical to decompose and form ZnO layers.

2.2.2(c) Chemical bath deposition

Aqueous base chemical bath deposition is the popular deposition method to grow ZnO nanomaterials in relatively low temperature (<100°C) and without further annealing process (Kumar et al., 2012, Chew et al., 2012). This advantage allows some low temperature resistance materials can be used in this deposition. Figure 2.4 represents a simple experimental setup for chemical bath deposition (CBD). This deposition can be assisted by applying electrochemical in this process to improve the growth. Zinc nitrate, $Zn(NO_3)_2$ as the main precursor to produce the ion species NO_3^- , and Zn^{2+} in alkaline medium. The following chemical equations (2.1) and (2.2) explain the deposition process (Sun et al., 2012).

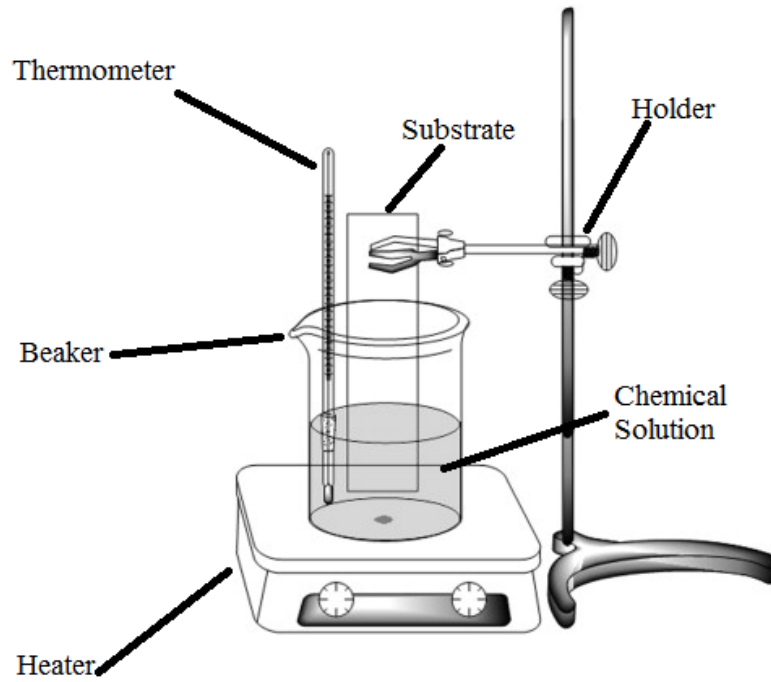
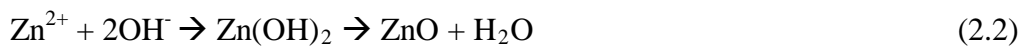


Figure 2.4: A simple experimental setup for chemical bath deposition (adapted from Serra et al., 2012).



To grow the well-aligned nanowires or nanorods, a seed layer of ZnO is required (Yu et al., 2011). The seed layer of ZnO can be prepared by sputtering or sol-gel method. The function of this seed layer is to prepare a platform and guide growth direction of ZnO nanowires.

2.2.3 Oxidation of metallic Zn

Oxidation of metallic Zn is a relatively simple route to produce ZnO thin film layers. Prior to oxidation process, a layer of metallic Zn can be prepared by vacuum thermal evaporation or sputtering (Figure 2.1). In principle, thermal evaporation happens when the solid source of metallic Zn usually in the form of granules is heated over its melting temperature in vacuum condition. During the evaporation process the high energy Zn atoms are transferred from the source to the substrate held above the source without any carrier gas. Figure 2.5 shows schematic diagram of vacuum thermal evaporation process. The background vacuum pressure usually pumped down to $\sim 10^{-6}$ Torr before evaporation process.

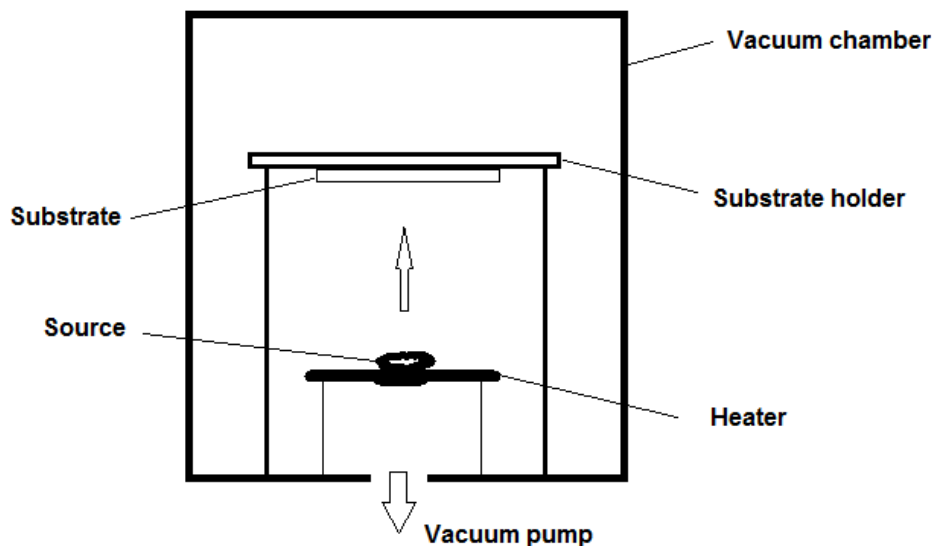


Figure 2.5 Schematic diagram of vacuum thermal evaporation process.

The temperature of the source is controlled by an electrical heater system. A boat made from tungsten, molybdenum, or tantalum is commonly used for the evaporation process. Granulated zinc was used as the source for metallic Zn films deposition (Hsu *et al.*, 2007). The coated Zn layer is transferred to a controlled furnace for the

oxidation process. The properties of the oxidized thin film layer depend on the oxidation parameters such as temperature, duration, and pressure (Wang et al., 2003, Hsu et al., 2007). The increase of oxygen contents during oxidation ensures the probability in growing nanomaterials is higher than thin film.

The investigation of ZnO nanowires growth mechanism based on resistive heating in the range of 673-1123K has been reported (Rackauskas et al., 2009). By using this method, the direction of the ZnO nanowires was found to grow along (110) and highest growth rate was observed at 803K. The Arrhenius plot obtained the growth activation energy related to Zn interstitial and vacancy migration and these also deduced to be limiting stage of the ZnO nanowires growth. Figure 2.6 shows the migration of Zn atoms towards the surface of ZnO layer through grain boundaries prior to the growth of ZnO nanowire via oxidation.

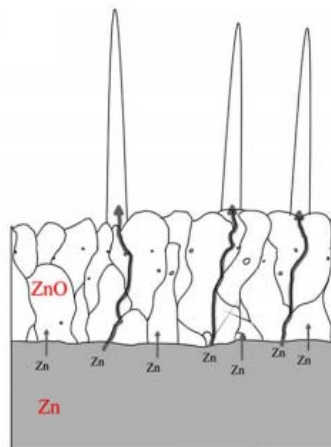


Figure 2.6: Schematic of ZnO nanowires growth mechanism (Rackauskas et al., 2009).

2.2.4 Solid-vapor phase deposition

Solid-vapor phase growth technique or thermal evaporation technique is a simple process for growing ZnO nanomaterials (Yousefi et al., 2012). In principle, the source materials are vaporized at certain temperature and then resulting vapor

phase condense on substrate by carrier gas. Figure 2.6 shows the schematic diagram of a typical solid-vapor phase system of growing ZnO nanomaterials. A quartz viewing window is usually available for monitoring during the growth process. The quality of ZnO nanomaterials can be affected by parameters such as temperature, pressure, gas ambient, distance from source, and substrate. Zinc powder or ZnO powder with graphite is usually used as starting source material. The carrier argon gas, Ar and reactive oxygen gas, O₂ are used to complete the mechanism as shown below:

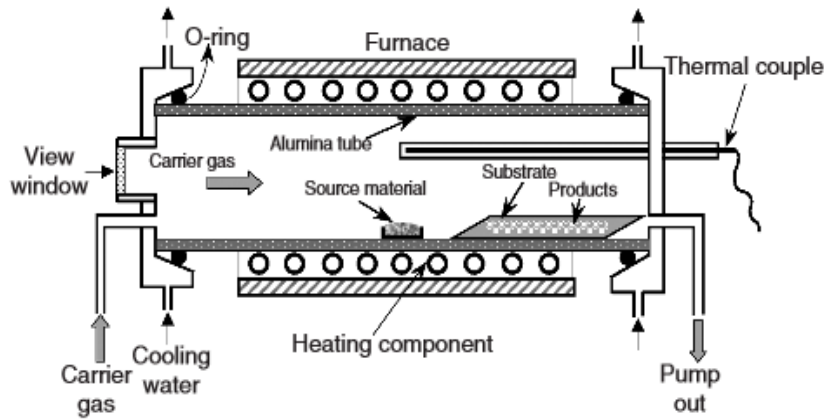


Figure 2.7: Schematic diagram of typical solid-vapor phase growth system (adapted from Wang et al. , 2004).

In typical conditions, a growth temperature of at least 900 °C is needed to break the Zn-O bond. Metal catalyst is often used to grow the well-aligned nanowires/ nanorods (Gao et al., 2003). A thin layer (~5 nm) of metal catalyst, which is usually Au, is coated on the substrate prior to solid-vapor phase process. The

disadvantage of this method is that the by-product (metal alloy on the tips of the nanomaterials) still remains inside the ZnO material.

2.2.5 Pulsed laser deposition

Pulsed laser deposition (PLD) has received good attention by researchers to grow wide bandgap semiconductor such as ZnO thin films (Liu et al., 2011, Sentosa et al., 2011). The basic principle of PLD is using heating from a pulse-laser source to vaporize the target material to be deposited as a thin film on a substrate. Figure 2.7 shows a schematic diagram of a typical pulsed laser deposition system used to grow ZnO thin films. A spherical stainless steel chamber is used as the vacuum chamber. The laser source (pulsed Nd-YAG or Excimer Laser) penetrates the quartz window to heat the target. The purpose of installing the lens in between the laser source and the quartz window is to focus and increase the intensity of the laser beam to heat up the target. Commonly used targets include ceramic sintered disc and pure metallic zinc due to cost consideration. Reactive gas (oxygen) was adjusted to a pressure of 50 to 300mTorr for ZnO when pure metallic zinc is used as target material. The influence of experimental parameters such as laser type or wavelength, target composition, substrate to target distance, the types of the substrates, background oxygen pressure, and the substrate temperature can be directly related to film quality (Vinay et al. , 2006).

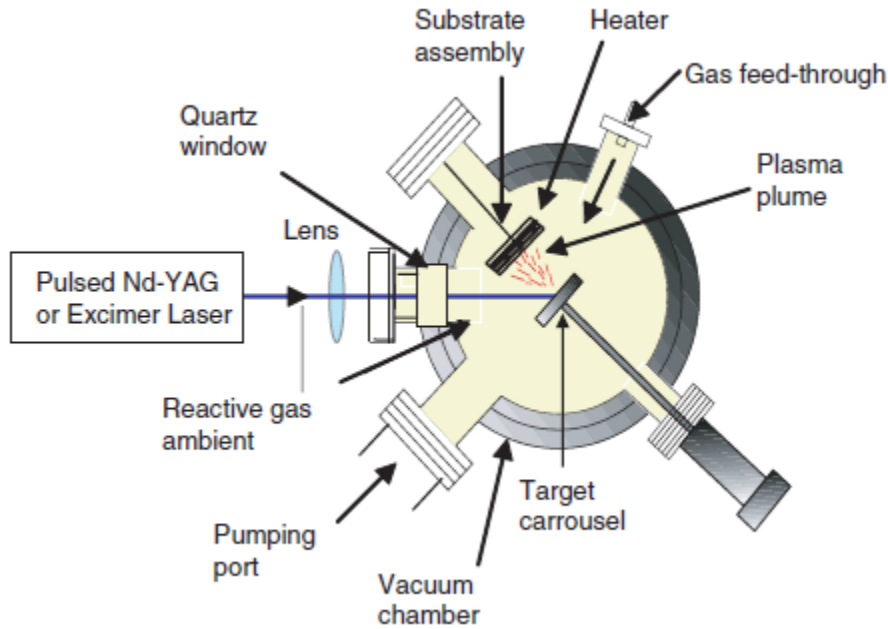


Figure 2.8 Schematic diagram of a pulsed laser deposition system (adapted from Gupta et al., 2006).

2.3 Doping and contacts of ZnO

Doping and contacts of ZnO are the important electrical properties of ZnO in electronic and optoelectronic applications. N- type or p-type semiconductor can be grown created by using different types of dopants. To measure this electrical characteristic, Hall effect is usually employed to determine the carrier type of semiconductors. The choice of metal contacts is another important parameter for devices fabrication. There are two major types of metal-semiconductor junctions to be considered: Ohmic and Schottky contacts.

Naturally, n-type ZnO are easily formed as compared to p-type ZnO due to the incorporation of hydrogen which will serve as a donor in ZnO during deposition (Kang et al., 2000). Therefore, the unintentionally-doped ZnO is always found to be n-type semiconductor. The group III elements aluminium (Al), gallium (Ga), and indium (In) are the common n-type dopants for ZnO. A low resistivity ZnO films

can be achieved with these dopants to become a good candidate for transparent conductive oxide materials and optoelectronic devices.

Group V elements (nitrogen-N, phosphorus-P, arsenide-As) and group I elements (lithium- Li) are source dopants usually used for p-type ZnO. P-type ZnO also can be produced by introducing more than one dopant source into ZnO (Zhang et al., 2007). There are some difficulties to produce a good quality of p-type ZnO. The preparation conditions such as temperature and the ratio of dopant can induce ZnO to behave as n-type ZnO (Wang et al., 2009, Zhang et al., 2007). The major disadvantage of p-type ZnO is the aging problem, which results in the change of its electrical properties. The actual problem for the electrical instability of ZnO is still well understood. Therefore, For ZnO devices which involve p-n junction, they always have a shorter lifetime as compared to their GaN counterpart.

Ohmic metal contacts on n-type ZnO, such as Al, and In metal contacts both with work function 4.2 eV they may form small Schottky barrier. The advantage of using these metal contacts is mainly due to the formation of non- alloyed Ohmic contacts without annealing (Kim et al., 2007). On another hand, Ohmic metal contacts on p-type ZnO require higher metal work function such as platinum (Pt~5.1 eV), palladium (~5.2 eV) and gold (Au~5.1 eV). Annealing process can be used to change the resistance at the interface between metal contacts and semiconductor.

High metal work function (Pt, Au, Pd) used to form Schottky metal contacts on n-type ZnO (Shao et al., 2010). However, Chromium (Cr) with the metal working ~ 4.5 eV was reported to form Schottky metal contacts on p-type ZnO (Stamataki et al., 2013).

2.4 Choice of substrates

There are many substrates for ZnO deposition such as amorphous glass, corning glass, quartz, sapphire, and silicon. However, the choice of substrates for obtaining high quality of ZnO layer remaining an issue. The type of substrate can be divided into two major groups: amorphous and crystalline substrate. For amorphous glass substrate the formation energy of crystallization of ZnO is higher than crystalline substrate. The initial growth of ~ 5 nm thickness normally is amorphous in nature, and with the increase of film thickness it will provide higher number of nucleating center due to the reduction of the energy (Gupta et al., 2006). Hence, growth of high crystalline ultrathin ZnO on amorphous glass has become another challenge.

Another factor such as lattice mismatch between ZnO and crystalline substrate also plays important roles. Due to the formation energy for the crystallization of ZnO, a smaller lattice mismatch could easily form highly c-axis oriented film as compare to higher lattice mismatch materials. For example, lattice mismatch between ZnO and c-plane sapphire was found ~18% (Ohtomo et al., 1999). Table 2.1 listed the summary of information for ZnO growth for variety growth techniques.

2.5 ZnO heterojunctions

As a wide and direct bandgap oxide semiconductor, the p-n junction of ZnO has received wide attention for optoelectronic device applications (Zhao et al., 2011). The ZnO homojunction is the most basic structure for ZnO p-n junction (Ryu et. al., 2003) and consists of n-type ZnO, p-type ZnO and related Ohmic contacts which shown in figure 2.8.

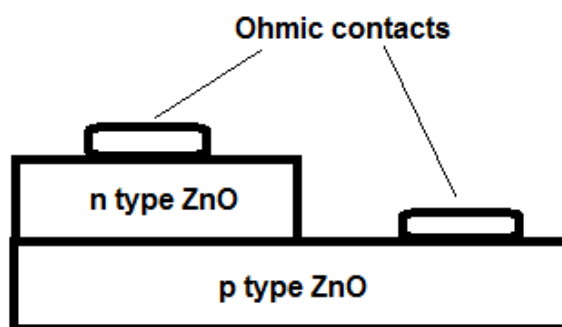


Figure 2.9: Schematic diagram of the basic ZnO homojunction.

However, it is difficult to grow p-type ZnO with stable electrical properties. This difficulty can be partly solved by replacing p-type ZnO with alternative wide bandgap semiconductors. One of the candidate materials is p-type GaN, due to the crystal structural (low lattice mismatch) and electrical (direct bandgap) properties that are similar to ZnO (Alivor et al., 2005).

Diamond is another suitable candidate to replace p type ZnO for fabricating a heterojunction. It should be noted that high quality n-type diamond is hard to be fabricated but stable p-type diamond can be fabricated relatively easier by doping it with boron. (Koizumi et al., 2001). Wang *et al.* reported a good rectifying characteristic as well as high transmission at visible regions for the ZnO thin film on diamond p-n diode (Wang et al., 2004). Hence this heterojunction is a suitable candidate for UV detection due to the physical properties of ZnO and diamond.

2.6 ZnO based UV photodetector

Ultraviolet (UV) Schottky photodiodes, metal–semiconductor–metal (MSM) photodiodes (He et al., 2012) and p–n junction photodetectors (Huang et al., 2012, Lupan et al., 2011) are the common types of UV photodetectors. The UV

photodetectors have been widely used in pollution monitoring; water sterilization and space-to-space communications for propose commercial and military applications, respectively. The available photodetectors are Si-based and titanium dioxide (TiO_2) –based devices. However, the sensitive wavelength of TiO_2 materials to UV is limited to approximately 330 – 350 nm. One of the disadvantages of Si-based UV photodetector is low visible-blindness. Most UV sources include some amount of visible spectrum which means that the detector will receive signal from the source with increasing noise level. To increase the efficiency of the UV detector by lowering the noise to signal ratio, an optical filter is used to block the visible spectrum. By considering the intrinsic visible-blindness of the material, ZnO is promising candidate for this application. Based on literature review, the spectral response of ZnO is below 380 nm which is in ultraviolet type A range (400 - 315 nm or 3.10-3.94 eV) (Sun et al., 2010). Type IIb diamond has a low concentration of boron and is semiconducting without intentional doping. Type IIb diamond can be used as a stable p-type material for ZnO-based heterojunction for UV detection application.

From literatures, it was known those ZnO single crystals grown by hydrothermal technique can naturally have Zn-polar on top surface and O-polar on the bottom or vice versa (Ohshima et al., 2004, Endo et al., 2007). Both surfaces have shown significant difference in chemical properties. The Zn- or O-polar can be determined by etching in HCl which gives different morphology after being etched. As reported by Endo, Zn and O polarities exhibited significant morphological differences after etching (Endo et al., 2007). From figure 2.9, for Zn-polar side, hexagonal shaped cavities were found distributed whereas small pores were observed on the O-polar surface.

When UV photodetector was fabricated based on ZnO, it has been reported that different polarities demonstrated different responsivities (Endo et al., 2007). The high responsivity was recorded by the Schottky contacts (Pt) on Zn-polar surface, which was two times higher than that on the O-polar surface. This Schottky UV photodiode can be operated as a visible-blind UV sensor since the responsivity in the wavelength region larger than 380nm almost insignificant.

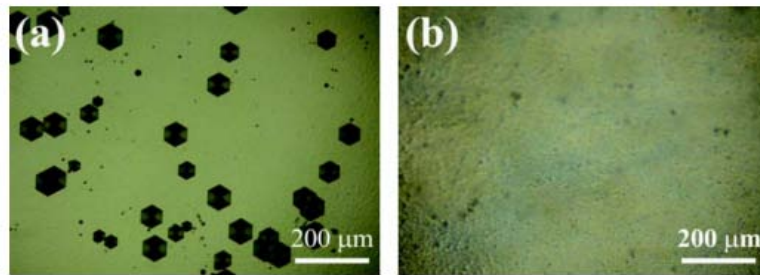


Figure 2.10: The optical images of a) Zn-polar, b) O-polar surface after etching (Endo et al., 2007).

Table 2.1: The summary of the selected growth techniques, precursors, morphological properties, and substrates for ZnO depositions.

Growth techniques	Sources/ precursors	Morphological structures/ thickness (nm)	Substrates	Remarks	References
R.F. magnetron sputtering	ZnO target	Thin film/ (130-300)	Glass	-	Schropp et al. 1989
Oxidation form metallic Zn	Zn target	Thin film/ (~200)	Fused silica	oxidation temperature : (300 - 1000 °C)	Cho et al., 1999
D.C. magnetron sputtering	Li:ZnO target	Thin film/ -	Sapphire, MgO, Quartz	-	Mohamed, et al., 2001
R.F. magnetron sputtering	Zn target	Thin film/ (~100)	Silicon, glass	Reactive gas: O ₂	Lee et al., 2002
Oxidation form metallic Zn	Zn target	Thin film/ (~200)	Silicon	oxidation temperature : (320 -	Wang et al., 2003

				1000 °C)	
R.F. magnetron sputtering	ZnO target	Thin film/ (~150)	Silicon	-	Lin <i>et al.</i> , 2004
R.F. and D.C. magnetron sputtering	Zn target	Thin films/ (~800)	Glass	Reactive gas: O ₂	Li <i>et al.</i> , 2004
Oxidation form metallic Zn	ZnO powder	Nanocrystals/-	Quartz	Vacuum evaporation to coat Zn metallic layer	Hsu, <i>et al.</i> , 2007
Spray pyrolysis	Zinc acetate, Aluminum nitrate, Ammonium acetate	Thin film/ (100 – 260)	Glass	Al-N co-doped p-type ZnO	Zhang <i>et al.</i> , 2007
Spray pyrolysis	Zinc nitrate	Thin film/ (~2300)	Silicon, Glass	-	P. Singh <i>et al.</i> , 2007
R.F. magnetron sputtering	Ga: Zn target	Thin film/ (~240)	GaN/ Sapphire	Ga doped n-type ZnO. Reactive gas: O ₂	Hwang <i>et al.</i> , 2009
Chemical bath depositions	Zinc nitrate	Nanorods/ -	GaN/ Sapphire	-	Alvi <i>et al.</i> , 2010
Vapor phase transport deposition	Zn powder	Nanowires/ (5000)	Ga:ZnO/ glass	-	Chen <i>et al.</i> , 2010
Sol-gel (Spin coating)	Zinc Naphthenate	Thin film/ (150-550)	Glass	-	Sahoo <i>et al.</i> , 2010
Sol-gel (dip-coating)	Zinc acetate, LiOH.H ₂ O, Al(NO ₃) ₃ .9H ₂ O	Thin film/ -	Silicon	Li-Al co-doped ZnO	Nain <i>et al.</i> , 2010
Sol-gel (Spin-coating)	Zinc acetate, Litium nitrate	Thin film/-	Silicon	Li doped p type ZnO	Wang <i>et al.</i> , 2009
Chemical bath depositions (electrodeposition)	Zinc nitrate	Nanowires/ (1000-5000)	F:SnO ₂ / Glass	-	Khajavi <i>et al.</i> , 2012
R.F. magnetron sputtering	ZnO target	Thin film/ (300)	B diamond/ Sigle crystal	-	Wang <i>et al.</i> , 2004